Control of a Quadcopter Using the Nested Saturation Approach

ARS5 Project Report

Ahmad SHOUR
Hasan KASSEM
Hussein LEZZAIK

Supervisor: Prof. Dr. Predro CASTILLO

University of Technology of Compiègne
23/01/2021

Contents

List of Figures

1 Introduction

Quadcopter, also known as quadrotor, is a helicopter with four rotors. The rotors are directed upwards and they are placed in a square formation with equal distance from the center of mass of the quadcopter. The quadrotor is one of the most complex flying machines. Its complexity is due to the versatility and maneuverability to perform many types of tasks. Quadcopters are used in surveillance, search and rescue, construction inspections and several other applications
In this project, we are particularly interested in controlling a mini rotorcraft having four rotors using the nested saturation approach.

Figure 1.1: The four-rotor rotorcraft

This four-rotor rotorcraft does not have a swashplate. In fact it does not need any blade pitch control. The collective input (or throttle input) is the sum of the thrusts of each motor. Pitch movement is obtained by increasing (reducing) the speed of the rear motor while reducing (increasing) the speed of the front motor. The roll movement is obtained similarly using the lateral motors. The yaw movement is obtained by increasing (decreasing) the speed of the front and rear motors while decreasing (increasing) the speed of the lateral motors. This should be done while keeping the total thrust constant.

We will present the model of a four-rotor rotorcraft whose dynamical model is obtained via a Lagrange approach.

The control algorithm is based on the nested saturation control strategy proposed by [1].

The report is organized as follows. The mathematical model is presented in Section II. Section III describes the control law design. In Section IV, we present numerical simulations and finally we conclude and analyze our final results in Section V.

1.1 Objectives

The main objective of this project is to propose a stabilization control algorithm for a quadrotor, based on the nested saturations. The main problem in designing such algorithms is to first obtain a model of the targeted system. In this case, we derive the mathematical model of our system using the Lagrange equations due to its ease of deriving the equations from conservation of energy.

2 Mathematical Model

In this section, we will study the mathematical model of the rotorcraft based on the **Lagrange** approach.

2.1 Generalized Coordinates

The generalized coordinates for the rotorcraft are:

$$q = (x, y, z, \psi, \theta, \phi) \tag{1}$$

where:

- $\xi = (x, y, z) \in R^3$ denotes the position of the center of mass of the helicopter relative to a fixed inertial frame
- $\zeta = (\psi, \theta, \phi) \in R^3$ are the Euler angles.
- ψ is the yaw angle around the z-axis.
- θ is the pitch angle around the modified y-axis.
- ϕ is the roll angle around the modified x-axis.

We define the Lagrangian as follows:

$$L(q, \dot{q}) = T_{trans} + T_{rot} - U \tag{2}$$

Where :

- $T_{trans} = \frac{1}{2} m \dot{\xi}^T \dot{\xi}$ is the translational kinetic energy.
- $T_{rot} = \frac{1}{2} \dot{\zeta}^T J \dot{\zeta}$ is the rotational kinetic energy.
- $U = mgz$ is the potential energy.

- z is the rotorcraft altitude.
- m is the mass of the rotorcraft.
- g is the acceleration due to gravity.

J is the inertia matrix of the rotorcraft, expressed in the inertial frame. $J = W^T I W$ with I being the quadcopter moment of inertia matrix in the body frame(represented according to the rotation axes sequence $z - y - x$) and W the transformation matrix of angular velocities of the quadcopter from inertial frame to the body frame, given by [2]:

$$W = \begin{pmatrix} -\sin(\theta) & 0 & 1 \\ \cos(\theta)\sin(\psi) & \cos(\psi) & 0 \\ \cos(\theta)\cos(\psi) & -\sin(\psi) & 0 \end{pmatrix} \tag{3}$$

2.2 Generalized Forces

The Euler Lagrange equations with external generalized forces is given by:

$$\frac{\partial}{\partial t}\frac{\partial L}{\partial \dot{q}} - \frac{\partial L}{\partial q} = F \tag{4}$$

where:

- $F = (F_\xi, \tau)$
- $\tau = (\tau_\phi, \tau_\theta, \tau_\psi)^T$ is the generalized moments.
- F_ξ is the translational force applied to the rotorcraft.

We ignore the small body forces because they are generally of a much smaller magnitude than the principal control inputs. Then:

$$F_\xi = R\hat{F} = R(0, 0, u)^T \tag{5}$$

Where:

- $u = f_1 + f_2 + f_3 + f_4$ is the resultant vertical force expressed in the body frame, which is one of our four control inputs. Note that there is only a vertical resultant force acting on the rotorcraft in the body frame.
- $f_i = k_i\omega_i^2$,with k_i being a constant and ω_i is the angular speed of the i^{th} motor.
- R is the transformation matrix representing the orientation of the rotorcraft given by (clockwise rotations are positive, $c_x \equiv \cos(x)$, and $s_x \equiv \sin(x)$):

$$R = \begin{pmatrix} c_\theta c_\psi & c_\theta s_\psi & -s_\theta \\ c_\psi s_\theta s_\phi - s_\psi c_\phi & s_\psi s_\theta s_\phi + c_\psi c_\phi & c_\theta s_\phi \\ c_\psi s_\theta c_\phi + s_\psi s_\phi & s_\psi s_\theta c_\phi - c_\psi s_\phi & c_\theta c_\phi \end{pmatrix} \tag{6}$$

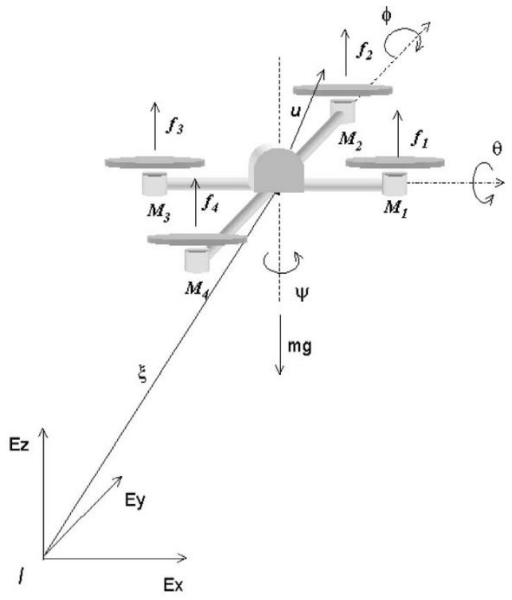

Figure 2.2.2: Schema of the four-rotor rotorcraft

We assume that the center of gravity is located at the intersection of the line joining motors M_1 and M_3 and the line joining motors M_2 and M_4 (see Figure 2.2.2). The generalized torques are thus:

$$\tau = (\tau_\psi, \tau_\theta, \tau_\phi)^T = (\sum_{i=1}^{4} \tau_{M_i}, (f_2 - f_4)l, (f_3 - f_1)l)^T \tag{7}$$

where l is the distance between the motors and the center of gravity, and τ_{M_i} is the moment produced by rotation of the motor M_i, i = 1, 2, 3, 4, around the center of gravity of the aircraft.
Since the Lagrangian contains no cross terms in the kinetic energy combining ζ and ξ, the Euler–Lagrange equation can be partitioned into the dynamics for the translational coordinates and rotational coordinates. We obtain:

$$m\ddot{\xi} + (0, 0, mg)^T = F_\xi \tag{8}$$

$$J\ddot{\zeta} + C(\zeta, \dot{\zeta})\dot{\zeta} = \tau \tag{9}$$

Where:

$$C(\zeta, \dot{\zeta})\dot{\zeta} = \dot{J}\dot{\zeta} - \frac{1}{2}\frac{\partial}{\partial \zeta}(\dot{\zeta}^T J \dot{\zeta}) \tag{10}$$

represent the Coriolis terms and gyroscopic and centrifugal terms.
Since out last three control input are τ, we propose the following virtual control inputs:

$$\tilde{\tau} = J^{-1}(\tau - C(\zeta, \dot{\zeta})\dot{\zeta}) \tag{11}$$

2.3 Final Model

Using equations (8),(9) along with (5),(6), and (11), the nonlinear equations modeling our systems are:

$$m\ddot{x} = -u\sin(\theta) \tag{12}$$
$$m\ddot{y} = u\cos(\theta)\sin(\phi) \tag{13}$$
$$m\ddot{z} = u\cos(\theta)\cos(\phi) - mg \tag{14}$$
$$\ddot{\psi} = \tilde{\tau}_\psi \tag{15}$$
$$\ddot{\theta} = \tilde{\tau}_\theta \tag{16}$$
$$\ddot{\phi} = \tilde{\tau}_\phi \tag{17}$$

Where $(u, \tilde{\tau}_\psi, \tilde{\tau}_\theta, \tilde{\tau}_\phi)$ represents the system input.

3 Control Laws and Stability

In order to control such systems, special care must be given to the design of the controller in order to compensate for the lost dynamics.

The quadcopter is controlled by adjusting the angular velocities of the rotors which are spun by electric motors. These inputs are mapped to our four virtual inputs $(u, \tilde{\tau}_\psi, \tilde{\tau}_\theta, \tilde{\tau}_\phi)$. We will use the main thrust u to stabilize the altitude of the rotorcraft, then we stabilize the yaw angle using $\tilde{\tau}_\psi$. Then, $\tilde{\tau}_\theta$ and $\tilde{\tau}_\phi$ are used to control (x, θ) and (y, ϕ) respectively.

3.1 Altitude Control and Stability

If we set:

$$u = (mv + mg)\frac{1}{\cos\theta\cos\phi} \tag{18}$$

equation (14) will become:

$$\ddot{z} = v \tag{19}$$

Letting $e_z = z - z_d$ with z_d being a desired reference for z (can be constant or time-varying), we propose:

$$v = \ddot{z_d} - k_{z1}(\dot{z} - \dot{z_d}) - k_{z2}(z - z_d) \tag{20}$$

with $k_{z1}, k_{z2} > 0$, which turns (19) into:

$$\ddot{e_z} = -k_{z1}\dot{e_z} - k_{z2}e_z \tag{21}$$

To prove stability, propose the following Lyapunov candidate function:

$$V = \frac{1}{2}k_{z2}e_z^2 + \frac{1}{2}\dot{e_z}^2$$

Which is a positive definite function in e_z. Then,

$$\begin{aligned}\dot{V} &= k_{z2}e_z\dot{e_z} + \dot{e_z}\ddot{e_z} \\ &= k_{z2}e_z\dot{e_z} + \dot{e_z}(-k_{z1}\dot{e_z} - k_{z2}e_z) \\ &= -k_{z1}\dot{e_z}^2\end{aligned}$$

Which validates that the system globally converges: $e_z \to 0$ and $\dot{e_z} \to 0$.
Note that we will choose our desired trajectories to have z linear with time. This will imply $\ddot{z_d} = 0$ and hence $v \to 0$.

3.2 Yaw Control and Stability

Equation (15) has the same form as equation (19), which implies that the control input:

$$\tilde{\tau_\psi} = \ddot{\psi_d} - k_{\psi 1}(\dot{\psi} - \dot{\psi_d}) - k_{\psi 2}(\psi - \psi_d) \tag{22}$$

will stabilize ψ using the same analysis from the previous section, where ψ_d is the desired yaw angle profile.

3.3 (y, ϕ) Control and Stability

After applying the control input given by (18) for a short period of time, u reduces to:

$$u \approx \frac{0 + mg}{\cos\theta\cos\phi} \tag{23}$$

substituting this into (13), and knowing that ϕ will be kept small enough:

$$\ddot{y} = g\tan\phi \approx g\phi \tag{24}$$

Using (17) and differentiating the above equation twice:

$$y^{(iv)} = g\tilde{\tau_\phi} \tag{25}$$

Let $e_y = y - y_d$ where y_d is the desired profile of y:

$$\begin{aligned}\dot{e_y} &= \dot{y} - \dot{y_d} \\ \ddot{e_y} &= \ddot{y} - \ddot{y_d} \\ &= g\phi - \ddot{y_d} \\ e_y^{(3)} &= g\dot{\phi} - y_d^{(3)} \\ e_y^{(iv)} &= g\ddot{\phi} - y_d^{(iv)} \\ &= g\tilde{\tau_\phi} - y_d^{(iv)}\end{aligned}$$

Let $\bar{\tau}$ be such that:

$$e_y^{(iv)} = g\tilde{\tau_\phi} - y_d^{(iv)} = \bar{\tau} \tag{26}$$

Now, we will find the control input $\bar{\tau}$ that stabilizes (26).
Consider the Lyapunov function $V_1 = \frac{1}{2}(e_y^{(3)})^2$. Hence:

$$\dot{V}_1 = e_y^{(3)} e_y^{(iv)} = e_y^{(3)} \bar{\tau} \tag{27}$$

Propose:

$$\bar{\tau} = -\sigma_{m_{\phi 1}}(e_y^{(3)} + \gamma_1) \tag{28}$$

where $|\gamma_1| \leq m_{\phi 2}$. $m_{\phi 1}, m_{\phi 2}$ are positive reals, and σ_k is a saturation function defined by:

$$\sigma_k(x) = \begin{cases} x & \text{if } |x| \leq k \\ k\,\mathrm{sgn}(x) & \text{otherwise} \end{cases} \tag{29}$$

Now suppose that $|e_y^{(3)}| \geq m_{\phi 2}$. Then, $(e_y^{(3)} + \gamma_1)$ has the same sign as $e_y^{(3)}$. This means that $\mathrm{sgn}(\dot{V}_1) = -\mathrm{sgn}(e_y^{(3)})\mathrm{sgn}(e_y^{(3)}) = -1$. Hence, $|e_y^{(3)}|$ will decrease and, after some time, will reach $|e_y^{(3)}| \leq m_{\phi 2}$. In that case, we will have $|e_y^{(3)} + \gamma_1| \leq 2m_{\phi 2}$.
Taking $m_{\phi 1} \geq 2m_{\phi 2}$, our control input will become:

$$\bar{\tau} = -(e_y^{(3)} + \gamma_1) \tag{30}$$

Now let $\nu_1 = e_y^{(3)} + \dot{e_y}$ and define $V_2 = \frac{1}{2}\nu_1^2$. We have:

$$\begin{aligned} \dot{V}_2 &= \nu_1 \dot{\nu_1} \\ &= \nu_1(e_y^{(iv)} + e_y^{(3)}) \\ &= \nu_1(\bar{\tau} + e_y^{(3)}) \\ &= \nu_1(-e_y^{(3)} - \gamma_1 + e_y^{(3)}) \\ &= -\nu_1\gamma_1 \end{aligned}$$

let $\gamma_1 = \sigma_{m_{\phi 2}}(\nu_1 + \gamma_2)$, where $|\gamma_2| \leq m_{\phi 3}$. By similar analysis as before, that if $|\nu_1| \geq m_{\phi 3}$, γ_1 will have the same sign as ν_1 and thus the negativity of $\dot{V}_2$ will make $|\nu_1|$ decrease and reach $|\nu_1| \leq m_{\phi 3}$ after some time. And, taking $m_{\phi 2} \geq 2m_{\phi 3}$ will lead to:

$$\begin{aligned} \bar{\tau} &= -(e_y^{(3)} + \gamma_1) \\ &= -(e_y^{(3)} + \nu_1 + \gamma_2) \end{aligned}$$

Now let $\nu_2 = \nu_1 + \dot{e_y} + e_y$ and define $V_3 = \frac{1}{2}\nu_2^2$. We have:

$$\begin{aligned} \dot{V}_3 &= \nu_2 \dot{\nu_2} \\ &= \nu_2(\dot{\nu_1} + e_y^{(3)} + \dot{e_y}) \\ &= \nu_2(-\gamma_1 + \nu_1) \\ &= \nu_2(-(\nu_1 + \gamma_2) + \nu_1) \\ &= -\nu_2\gamma_2 \end{aligned}$$

let $\gamma_2 = \sigma_{m_{\phi 3}}(\nu_2 + \gamma_3)$, where $|\gamma_3| \leq m_{\phi 4}$. By similar analysis as before, that if $|\nu_2| \geq m_{\phi 4}$, γ_2 will have the same sign as ν_2 and thus the negativity of $\dot{V}_3$ will make $|\nu_2|$ decrease and reach $|\nu_2| \leq m_{\phi 4}$

after some time. And, taking $m_{\phi 3} \geq 2m_{\phi 4}$ will lead to:

$$\begin{aligned}\bar{\tau} &= -(e_y^{(3)} + \nu_1 + \gamma_2) \\ &= -(e_y^{(3)} + \nu_1 + \nu_2 + \gamma_3)\end{aligned}$$

Now let $\nu_3 = \nu_2 + \dddot{e_y} + 2\dot{e_y} + e_y$ and define $V_4 = \frac{1}{2}\nu_3^2$. We have:

$$\begin{aligned}\dot{V_4} &= \nu_3\dot{\nu_3} \\ &= \nu_3(\dot{\nu_2} + e_y^{(3)} + 2\ddot{e_y} + \dot{e_y}) \\ &= \nu_3(-\gamma_2 + \nu_2) \\ &= \nu_3(-(\nu_2 + \gamma_3) + \nu_2) \\ &= -\nu_3\gamma_3\end{aligned}$$

let $\gamma_3 = \sigma_{m_{\phi 4}}(\nu_3)$. Then γ_3 will have the same sign as ν_3 and thus the negativity of $\dot{V_3}$ will make $|\nu_3|$ decrease and reach $|\nu_2| \leq m_{\phi 4}$ after some time. Then we will have $\dot{V_4} = -\nu_3^2$, which means that $\nu_3 \to 0$.
Now moving backwards in our analysis, we can see that after the time we achieve $\nu_3 \to 0$, the following will happen, sequentially:

- $\boldsymbol{\nu_3 \to 0}$
- $\gamma_3 \to 0$
- $\gamma_2 \to \nu_2$
- $\dot{V_3} \to -\nu_2^2$
- $\boldsymbol{\nu_2 \to 0}$
- $\gamma_2 \to 0$
- $\gamma_1 \to \nu_1$
- $\dot{V_2} \to -\nu_1^2$
- $\boldsymbol{\nu_1 \to 0}$
- $\gamma_1 \to 0$
- $\bar{\tau} \to -e_y^{(3)}$
- $\dot{V_1} \to -(e_y^{(3)})^2$
- $\boldsymbol{e_y^{(3)} \to 0}$
- $\boldsymbol{\dddot{e_y} \to 0}$ from $\nu_1 \to 0$
- $\boldsymbol{\dot{e_y} \to 0}$ from $\nu_2 \to 0$
- $\boldsymbol{e_y \to 0}$ from $\nu_3 \to 0$

Which ensures our system stability. Hence, using the definitions of ν_1, ν_2, and ν_3, our control input will be:

$$\begin{aligned}\bar{\tau} = -\sigma_{m_{\phi 1}}(e_y^{(3)} + \\ \sigma_{m_{\phi 2}}(e_y^{(3)} + \ddot{e_y} + \\ \sigma_{m_{\phi 3}}(e_y^{(3)} + 2\ddot{e_y} + \dot{e_y} + \\ \sigma_{m_{\phi 4}}(e_y^{(3)} + 3\ddot{e_y} + 3\dot{e_y} + e_y))))\end{aligned}$$

with $\tilde{\tau}_\phi = \frac{1}{g}(\bar{\tau} + y_d^{(iv)})$.

3.4 (x, θ) Control and Stability

Using (23) in (12), and knowing that θ and ϕ will be kept small enough, we obtain:

$$\ddot{x} \approx -g\theta \tag{31}$$

Now observe that the equations couples (31),(16) and (24),(17) are similar, differing only by the sign behind g. Thus, we can treat the system of (x, θ) like the already analyzed system of (y, ϕ) by taking $g \equiv -g$, which leads to the following control law:

$$\begin{aligned}\bar{\bar{\tau}} = -\sigma_{m_{\theta 1}}(e_x^{(3)} + \\ \sigma_{m_{\theta 2}}(e_x^{(3)} + \ddot{e_x} + \\ \sigma_{m_{\theta 3}}(e_x^{(3)} + 2\ddot{e_x} + \dot{e_x} + \\ \sigma_{m_{\theta 4}}(e_x^{(3)} + 3\ddot{e_x} + 3\dot{e_x} + e_x))))\end{aligned}$$

with the following conditions similar as those presented in the previous section:

- $\tilde{\tau}_\theta = \frac{1}{-g}(\bar{\bar{\tau}} + x_d^{(iv)})$
- x_d is the desired profile of x and $e_x = x - x_d$
- $m_{\theta 1}, m_{\theta 2}, m_{\theta 3}, m_{\theta 4}$ are positive reals with $m_{\theta 1} \geq 2m_{\theta 2} \geq 4m_{\theta 3} \geq 8m_{\theta 4}$

4 Numerical Simulations

We presented a trajectory tracking controller design for a mini rotor-craft having four rotor after, getting it's dynamic model via a Lagrange approach. We tested the proposed controller in MATLAB with various initial conditions, gains, and trajectory profiles. These experiments show that the mini-aircraft is able to track satisfactorily the desired trajectory.
We carefully chose the design parameters according to typical quadcopters. The following settings were used for our simulations:

- Mass: $m = 1.63kg$
- Gravitational acceleration: $g = 10N/kg$
- Moments of inertia: $I_{xx} = 0.0093kg.m^2, I_{yy} = 0.0092kg.m^2, I_{zz} = 0.0151kg.m^2$
- Sampling time: $\Delta t = 50ms$
- Simulation time: $48s$

and the following gains were used:

$k_{z1} = 2.4$	$m_{\phi 1} = 8$	$m_{\theta 1} = 8$
$k_{z2} = 0.4$	$m_{\phi 2} = 4$	$m_{\theta 2} = 4$
$k_{\psi 1} = 2.4$	$m_{\phi 3} = 2$	$m_{\theta 3} = 2$
$k_{\psi 2} = 2.4$	$m_{\phi 4} = 1$	$m_{\theta 4} = 1$

Table 1: Simulation Gains

We will present the different trajectories investigated.

4.1 Constant Reference

We set the target position of the quadcopter to be $(2, 3, 4)$. We started the simulation with initial position at the origin, all angles and angular velocities were set to zero, except the yaw angle was set to $\frac{\pi}{3}$. The following figure illustrates the convergence of our system.

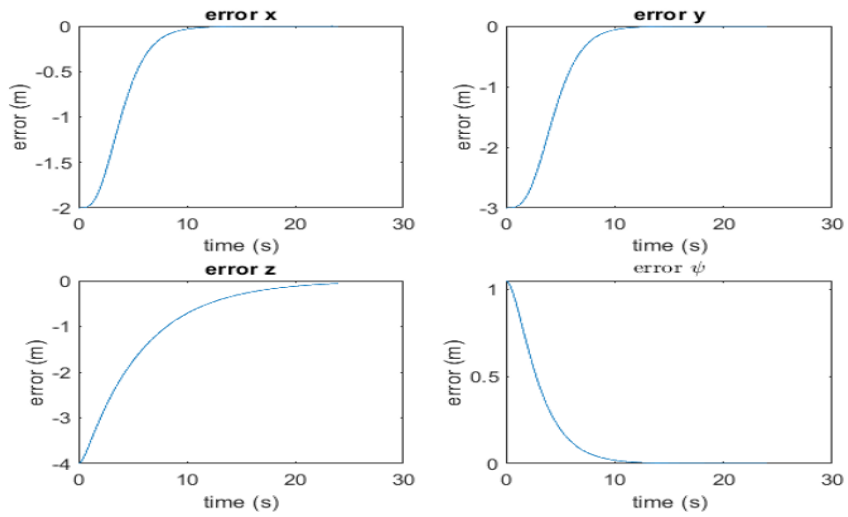

Figure 4.1.3: System errors with fixed desired position

The real inputs (thrust and torques) were calculated based on the virtual ones, and were plotted in the following figure:

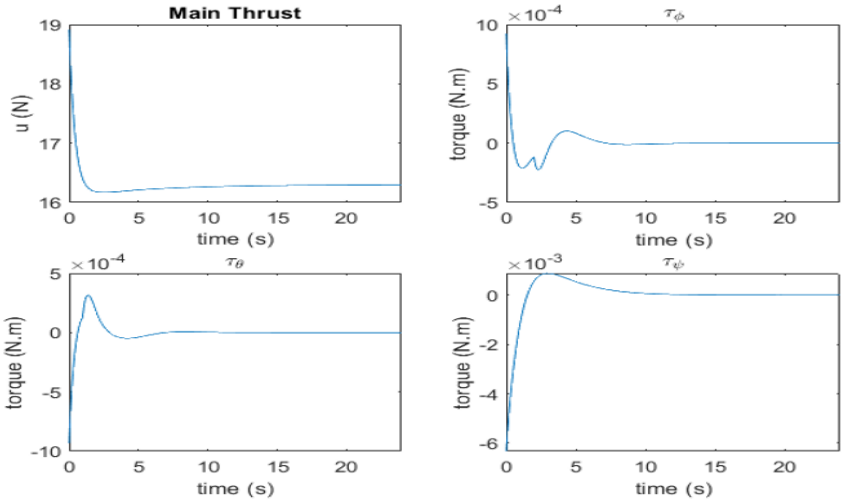

Figure 4.1.4: System inputs with fixed desired position

These inputs can assure how realistic is the control law, and how the saturation functions limited these inputs in the expense of a little delay of system convergence.

4.2 Cylinder Trajectory

We then set a desired trajectory profile rather than a fixed reference. The equations of the cylindrical trajectory used is given by:

$$\begin{cases} x = 1 + \cos(t/2) \\ y = 1 + \sin(t/2) \\ z = t/6 \end{cases}$$

We started the simulation with initial position at the $(0, 0, 0)$, all angles and angular velocities were set to zero, except the yaw angle was set to $\frac{\pi}{3}$. The following figure illustrates the convergence of our system.

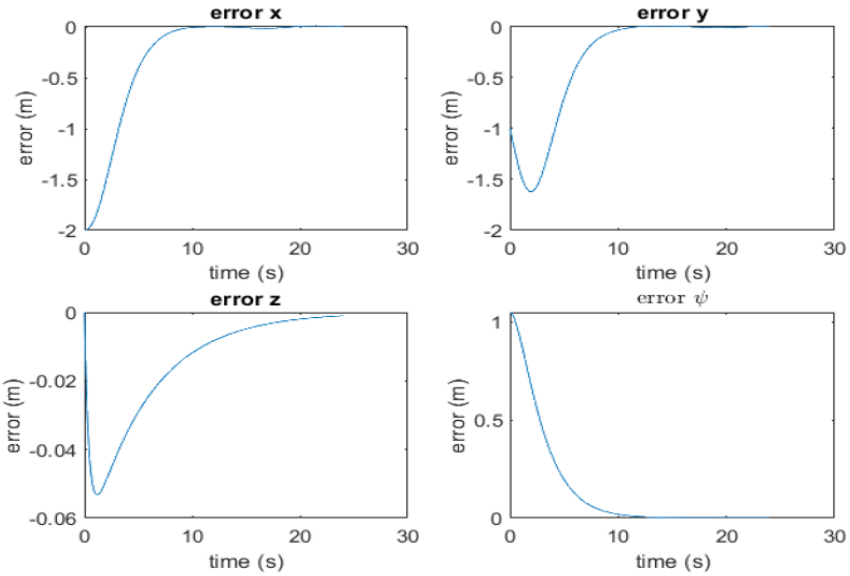

Figure 4.2.5: System errors with cylinder motion

The real inputs are also plotted to keep track of how large they are, and we present the 3D plot of the desired trajectory and the quadcopter's:

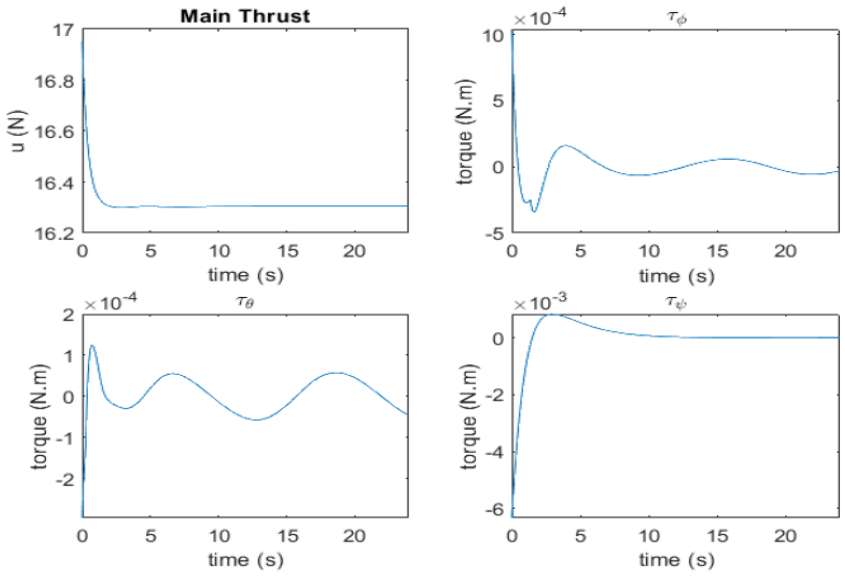

Figure 4.2.6: System inputs with cylinder motion

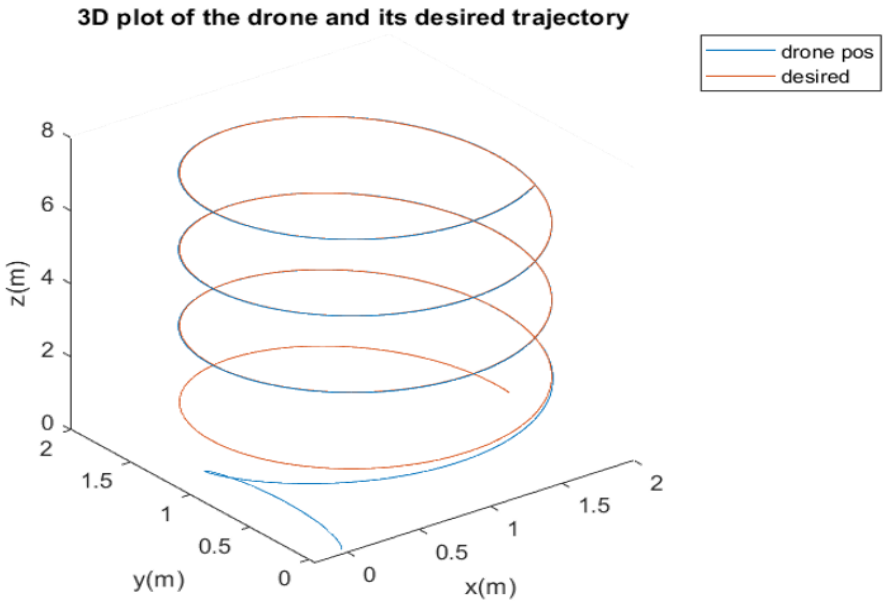

Figure 4.2.7: Quadcopter trajectory and the desired cylindrical one.

4.3 Spiral Trajectory

Now this trajectory seems to be interesting in terms of system convergence. The equations of the spiral trajectory used is given by:

$$\begin{cases} x = 1 + \frac{t}{6}\cos(t/2) \\ y = 1 + \frac{t}{6}\sin(t/2) \\ z = t/6 \end{cases}$$

We started the simulation with initial position at the $(2, 1, 0)$, all angles and angular velocities were set to zero, except the yaw angle was set to $\frac{\pi}{3}$. Simulation time was extended to $88s$ to illustrate how the system has some difficulty in being stable when the spiral radius gets larger. The following figure shows the system errors.

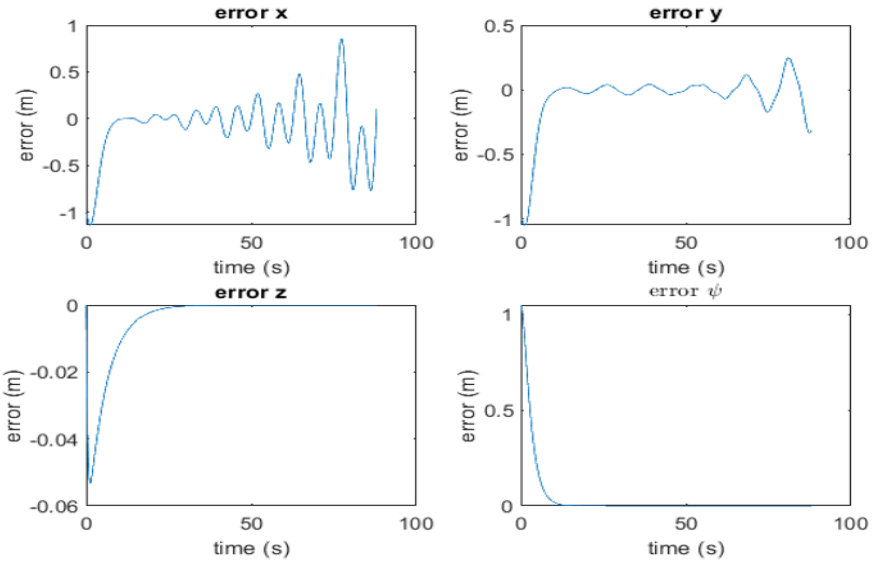

Figure 4.3.8: System errors with spiral motion

We can notice how the error in x started to stabilize around $t = 20s$. Noticing that our trajectory's acceleration in x and y is proportional to time, we can find that the ϕ angle will not be near zero, the condition we built our controller on. This argument is justified by the fact that, in section 3.3, we forced $\ddot{e_y} \to 0$, which is equivalent to $(g\phi - \ddot{y_d}) \to 0$ by the definition of e_y. This means that we should impose a limit on our desired trajectory accelerations in order guarantee the validity of our controller.
The real inputs are also plotted to see how the system inputs react to following the spiral:

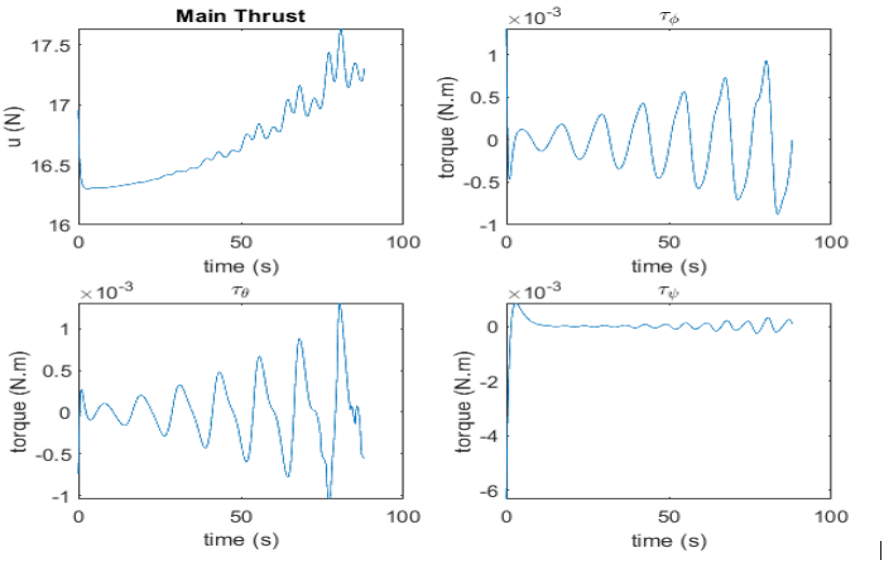

Figure 4.3.9: System inputs with spiral motion

We can see higher and more fluctuating torque inputs than those used in the previous trajectories, and a trend of increasing thrust demand.
The plot below also shows the 3D desired trajectory and the one traversed by the quadcopter:

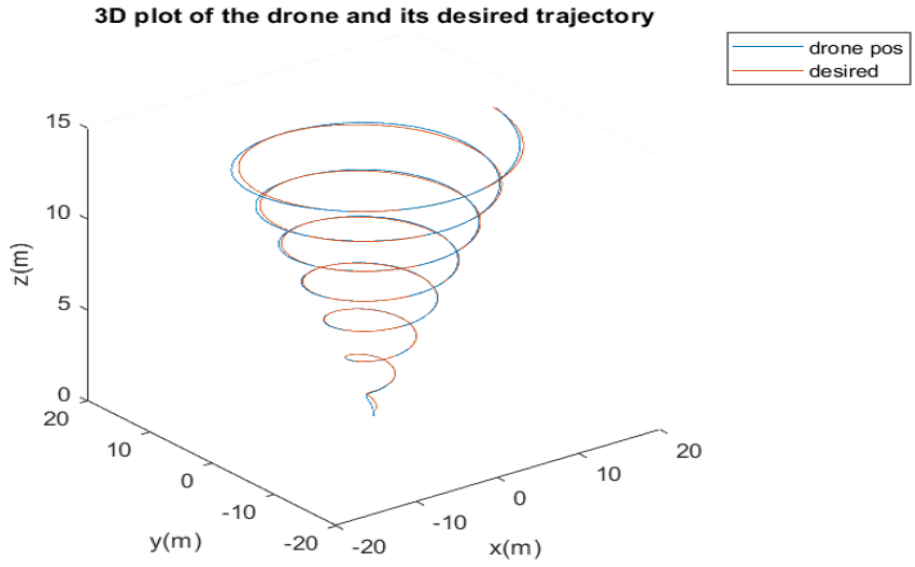

Figure 4.3.10: Quadcopter trajectory and the desired spiral one.

4.4 Adding Noise

We tested our system with simulated noise, to study the robustness of our control algorithm. The noise applied to each control input of $(v, \tilde{\tau}_\psi, \tilde{\tau}_\theta, \tilde{\tau}_\phi)$ is modelled as white noise with variance equals to double the input's value. The test was performed on the same cylinder trajectory experimental settings. We kept increasing noise value until we saw significant effect on our system. The following figures show the system errors and the main inputs when noise is applied.

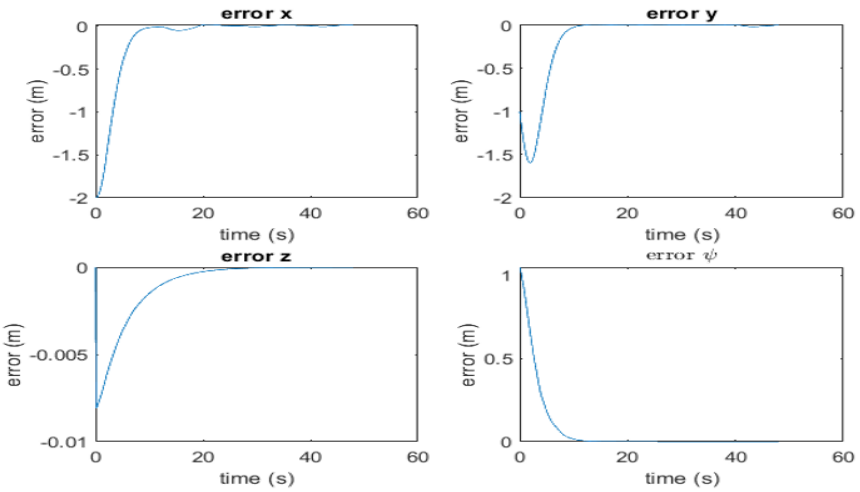

Figure 4.4.11: System errors with added noise

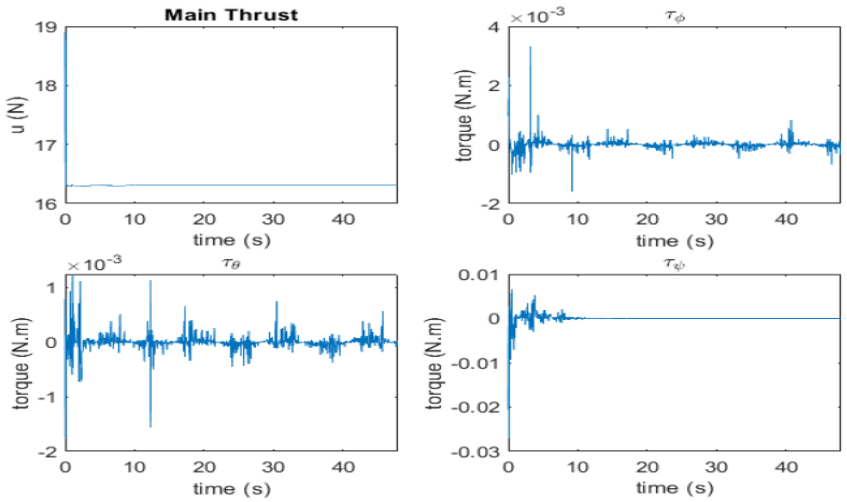

Figure 4.4.12: System inputs with added noise

As we can see, the system still converges. The following plot also shows the 3D behaviour:

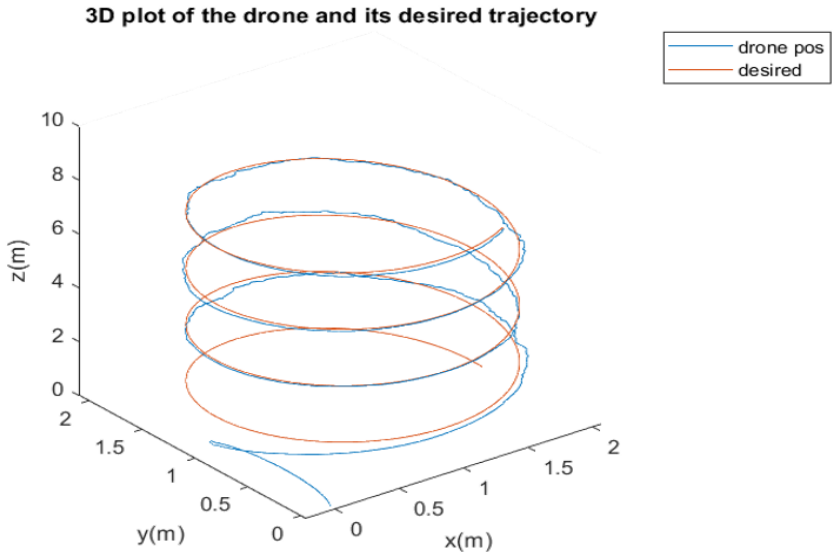

Figure 4.4.13: Quadcopter noisy trajectory and the desired cylindrical one.

5 Conclusions

In this project,we have proposed a stabilization control algorithm for a mini rotorcraft having four rotors. The dynamic model of the rotor- craft was obtained via a Lagrange approach and the proposed control algorithm is based on nested saturation. The results show the convergence of our proposed controller.

We have noticed how the controller may fail for large acceleration values of the states x and y, and that was due to assumptions on small pitch and roll angles during the controller design, not because of limited input energy. So, further work is needed to develop more robust controller that is not limited by trajectories properties. Nevertheless, the presented trajectories were tracked successfully.

References

[1] A. R. Teel, "Global stabilization and restricted tracking for multiple in- tegrators with bounded controls," Syst. Control Lett., 1992.

[2] Castillo, P.; Lozano, R.; Dzul, A. Stabilization of a mini-rotorcraft having four rotors. 2004 IEEE/RSJInternational Conference on Intelligent Robots and Systems (IROS) (IEEE Cat. No.04CH37566)2004,3, 2693–2698.